World Journal of Advanced Engineering Technology and Sciences
eISSN: 2582-8266
Cross Ref DOI: 10.30574/wjaets
Journal homepage: https://wjaets.com/

(RESEARCH ARTICLE)

Check for updates

A Lagrange Galerkin Scheme for the Numerical Stability of the Shallow Water Equations with the Transmission Boundary Condition through Energy Estimates

Md. Masum Murshed *

Department of Mathematics, University of Rajshahi, Rajshahi-6205, Bangladesh.

World Journal of Advanced Engineering Technology and Sciences, 2024, 12(02), 832–840

Publication history: Received on 09 July 2024; revised on 15 August 2024; accepted on 17 August 2024

Article DOI: https://doi.org/10.30574/wjaets.2024.12.2.0350

Abstract

This paper presents a study on the shallow water equations (SWEs) with specified Dirichlet and transmission boundary conditions (TBC). A Lagrange-Galerkin (LG) scheme is employed for numerical discretization. The stability of the solution is analyzed using energy estimates. The results shows that the total energy generally decreases over time and that the energy derivatives are non-positive, which confirms the numerical stability of the solution.

Keywords: Lagrange Galerkin Scheme; Numerical Stability; Shallow Water Equations; Transmission Boundary Condition; Energy Estimates

1. Introduction

The SWEs can be regarded as a coupled system consisting of a pure convection equation for the function ϕ, representing the total wave height, and a simplified Navier-Stokes equation for the velocity $u = (u_1, u_2)^T$, derived by averaging values in the x_3-direction. These equations are frequently used to simulate events such as tsunamis or storm surges in bays. During such simulations, special boundary conditions are necessary at the open sea boundaries to prevent artificial reflections when waves propagate towards these boundaries (see Figure 1). To address this, a TBC, as described in [5], is applied on Γ_T, the boundaries in the open sea. This TBC effectively removes artificial reflections and is defined by:

$$u(x,t) = c(x)\frac{\eta(x,t)}{\phi(x,t)}n(x), \qquad (1)$$

where $c(x)$ is a positive function, $\eta(x,t) = \phi(x,t) - \zeta(x)$ represents the elevation from the reference height for a given depth function ζ, and $n(x)$ is the unit normal vector at the boundary.

Numerous studies, including [1–3, 7–14], have examined surge predictions due to tropical storms in the Bay of Bengal, which encompasses the coast of Bangladesh and the east coast of India. These studies typically employ radiation-type boundary conditions for the open sea boundaries, which are similar to the TBC described in [4]. According to [6], TBCs provide more accurate results for SWEs simulations than radiation boundary conditions. However, it is important to note that many of these studies focus on numerical results without confirming the mathematical stability of the model with such boundary conditions.

* Corresponding author: Md. Masum Murshed *
Department of Mathematics, University of Rajshahi, Rajshahi-6205, Bangladesh.

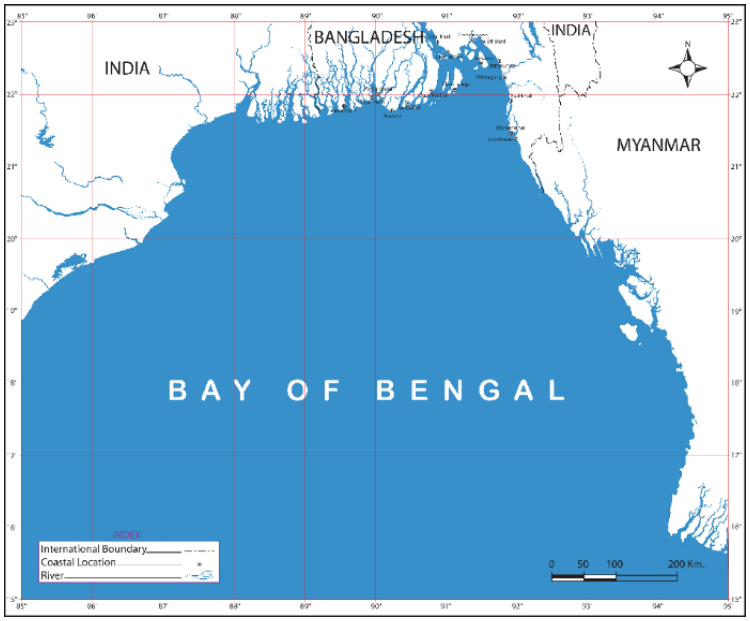

Figure 1 The Bay of Bengal and the coastal region of Bangladesh

In [5], both theoretical and numerical stability analyses of the SWEs using TBCs were performed using finite difference methods (FDM). While FDM is suitable for rectangular or square domains, real-world domains are often irregular. For these complex shapes, the finite element method (FEM), especially with triangular meshes, is more appropriate.

In computations, the "upwind point" $x - u^k(x)\Delta t$ is used. If this point lies outside the domain, the nearest boundary value of ϕ^k is used. The Lagrange Galerkin Method (LGM), which is an FEM based on time discretization of the material derivative, $\frac{\phi^{k+1}(x)-\phi^k(x-u^k(x)\Delta t)}{\Delta t}$, is effective for these computations. Unlike FDM, which fails without boundary data for ϕ^{k+1} if $u^{k+1} \cdot n < 0$, LGM can work without boundary data under such conditions.

This study investigates the stability of the SWEs with TBCs in terms of suitable energy estimates. The numerical confirmation of stability is achieved using the LGM with triangular meshes. These results will help to develop an efficient storm surge prediction model implementing FEM.

1.1. Statement of the problem

Following [5], the mathematical problem is formulated for this paper. Let $\Omega \subset \mathbb{R}^2$ be a bounded domain and T a positive constant. We consider the problem of finding (ϕ, u): $\overline{\Omega} \times [0,T] \to \mathbb{R} \times \mathbb{R}^2$ such that

$$\begin{cases} \dfrac{\partial \phi}{\partial t} + \nabla \cdot (\phi u) = 0 & in\ \Omega \times (0,T), \\ \rho\phi\left[\dfrac{\partial u}{\partial t} + (u \cdot \nabla)u\right] - 2\mu\nabla \cdot \big(\phi D(u)\big) + \rho g \phi \nabla \eta = 0 & in\ \Omega \times (0,T), \\ \phi = \eta + \zeta & in\ \Omega \times (0,T), \end{cases} \tag{2}$$

with boundary conditions

$$u = 0 \qquad \text{on} \quad \Gamma_D \times (0,T), \tag{3}$$

$$u = c\frac{\eta}{\phi}n \qquad \text{on} \quad \Gamma_T \times (0,T), \tag{4}$$

and initial conditions

$$u = u^0, \quad \eta = \eta^0 \qquad \text{in } \Omega, \text{ at } t = 0, \tag{5}$$

where ϕ is the total wave height, $u = (u_1, u_2)^T$ is the velocity, $\eta: \overline{\Omega} \times [0,T] \to \mathbb{R}$ is the water level relative to the reference height, $\zeta(x) > 0$ $(x \in \overline{\Omega})$ is the depth of water from the reference height (see Figure 2). The strain-rate tensor $D(u) := (\nabla u + (\nabla u)^T)/2$, and n is the unit outward normal vector to the boundary of Ω. The boundary $\Gamma := \partial\Omega$ consists of two non-overlapping parts, Γ_D and Γ_T, i.e., $\overline{\Gamma} = \overline{\Gamma}_D \cup \overline{\Gamma}_T$, $\Gamma_D \cap \Gamma_T = \emptyset$. The subscripts D and T denote Dirichlet and transmission boundaries, respectively. The constants $\rho > 0$ and $\mu > 0$ represent the density and viscosity of water, respectively, while $g > 0$ is the acceleration due to gravity, and $c(x) := c_0\sqrt{g\zeta(x)}$ with a positive constant c_0. In the rest of paper $\zeta \in C^1(\overline{\Omega})$ is assumed.

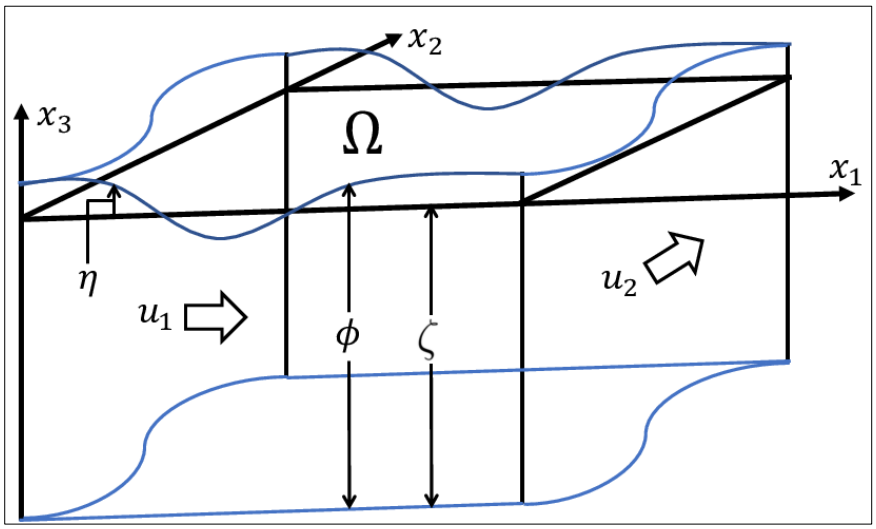

Figure 2 Model domain (see [5])

1.2. Energy estimate

According to [5], for a solution of (2) the total energy E(t) at time t ∈ [0, T] is defined by

$$E(t) := E_1(t) + E_2(t), \tag{6}$$

where $E_1(t) := \int_\Omega \frac{\rho}{2}\phi|u|^2\,dx$ is the kinetic energy and $E_2(t) := \int_\Omega \frac{\rho g|\eta|^2}{2}\,dx$ is the potential energy. Also, the derivative of the total energy (see [5]) is defined by

$$\frac{d}{dt}E(t) = \sum_{i=1}^{3} I_i(t;\Gamma) + I_4(t;\Omega), \tag{7}$$

where

$I_1(t;\Gamma) := -\frac{\rho}{2}\int_\Gamma \phi|u|^2\, u \cdot n\, ds,$

$I_2(t;\Gamma) := -\rho g \int_\Gamma \phi\eta\, u \cdot n\, ds,$

$I_3(t;\Gamma) := 2\mu \int_\Gamma \phi[D(u)n] \cdot u\, ds,$

and $I_4(t;\Omega) := -2\mu \int_\Omega \phi|D(u)|^2\, dx.$

1.3. LG scheme

Following [5] an LG scheme is considered as follows:

Let $\mathcal{T}_h = \{K\}$ be a triangulation of Ω, and M_h the so-called P1 (piecewise linear) finite element space. We set $\Psi_h := M_h$ for the water level η, and

$$V_h(\psi_h) \coloneqq \left\{ v_h \in M_h^2;\ \begin{matrix} v_h(P)=c(P)\frac{\psi_h(P)-\zeta(P)}{\psi_h(P)}n(P), & \forall P\colon node\ on\ \Gamma_T \\ v_h(Q)=0, & \forall Q\colon \text{node on } \Gamma_D \end{matrix} \right\}$$

for the velocity u. The LG scheme is to find $\left\{\left(\phi_h^k, u_h^k\right)\right\}_{k=1}^{N_T} \subset \Psi_h \times V_h$ such that, for $k = 1, \dots, N_T$,

$$\begin{cases} \displaystyle\int_\Omega \frac{\phi_h^k - \widetilde{\phi_h^{k-1}} \circ X_{1h}^{k-1}\gamma_h^{k-1}}{\Delta t}\psi_h dx = 0, & \forall \psi_h \in \Psi_h, \\ \displaystyle\rho\int_\Omega \phi_h^k \frac{u_h^k - \widetilde{u_h^{k-1}} \circ X_{1h}^{k-1}}{\Delta t}\cdot v_h dx + 2\mu\int_\Omega \phi_h^k D\left(u_h^k\right) : D(v_h)dx & \\ \displaystyle+\rho g\int_\Omega \phi_h^k \nabla\eta_h^k \cdot v_h dx = 0, & \forall v_h \in V_h, \\ \phi_h^k = \eta_h^k + \Pi_h^{\mathrm{FEM}}\zeta, & \end{cases} \tag{8}$$

where $X_{1h}^k(x) \coloneqq x - u_h^k(x)\Delta t$, $\gamma_h^k\colon \Omega \to \mathbb{R}$ is defined by

$$\gamma_h^k(x) \coloneqq \det\left(\frac{\partial X_{1h}^k(x)}{\partial x}\right),$$

the symbol "$\circ$" represents the composition of functions, i.e., $\left[v_h \circ X_{1h}^k\right](x) \coloneqq v_h\left(X_{1h}^k(x)\right)$, $\Pi_h^{\mathrm{FEM}}\colon C\left(\overline{\Omega}\right) \to M_h$ is the Lagrange interpolation operator, and

$$\widetilde{\psi_h}(x) = \begin{cases} \psi_h(x), & x \in \overline{\Omega}, \\ \psi_h(P_x), & x \in \mathbb{R}^2 \setminus \overline{\Omega}, \end{cases}$$

where $P_x \in \Gamma$ is the "nearest" nodal point from x.

In each step, firstly, $\phi_h^k \in \Psi_h$ is obtained from the first equation of scheme (8). Secondly, $u_h^k \in V_h$ is obtained by using ϕ_h^k from the second equation.

In the first equation of (8), the idea of mass conservative LG scheme [15] is employed.

2. Numerical results

In this section numerical results are presented.

2.1. Problem setting

For the numerical computation we set $\Omega = (0, L)^2$ for a positive constant L, $T = 100$, $\zeta = a > 0$, $\mu = 1$, $g = 9.8 \times 10^{-3}$, $\rho = 10^{12}$, $\eta^0 = c_1 \exp(-100|x - p|^2)$ $(c_1 > 0, p \in \Omega)$. As the real domain is very large, we consider the length in km scale. So, the above values are in km (length), kg (mass) and s (time).

We consider five cases of Γ_T:

(i) $\Gamma_T = \emptyset$,
(ii) $\Gamma_T = \Gamma_{\mathrm{top}}$,
(iii) $\Gamma_T = \Gamma_{\mathrm{top}} \cup \Gamma_{\mathrm{right}} \cup \{(L, L)\}$,
(iv) $\Gamma_T = \Gamma_{\mathrm{top}} \cup \Gamma_{\mathrm{right}} \cup \Gamma_{\mathrm{left}} \cup \{(L, L)\} \cup \{(0, L)\}$,
(v) $\Gamma_T = \Gamma$,

for $\Gamma_{\mathrm{top}} \coloneqq \{(x_1, L); 0 < x_1 < L\}$, $\Gamma_{\mathrm{right}} \coloneqq \{(L, x_2); 0 < x_2 < L\}$, $\Gamma_{\mathrm{left}} \coloneqq \{(0, x_2); 0 < x_2 < L\}$, and set $\Gamma_D = \Gamma \setminus \Gamma_T$. For the above cases (ii)—(v), $c_0 = 0.9$ is taken following [5].

2.2. Numerical study of energy estimate

In this subsection, we study the stability of solutions to the problem (2)—(5) numerically by scheme (8) in terms of the energy $E(t)$ defined in (6).

The values of $E(t^k)$ and $I_i(t^k;\Gamma), i = 1,2,3, I_4(t^k;\Omega)$ are approximately computed by using solution $\{(u_h^k, \phi_h^k)\}_{k=1}^{N_T}$ with $\{\eta_h^k\}_{k=1}^{N_T}$ of scheme (8) as

$$E(t^k) \approx E_h^k := \int_\Omega \frac{\rho}{2}(\phi_h^k)|u_h^k|^2\,dx + \int_\Omega \frac{\rho g}{2}|\eta_h^k|^2 dx,$$

$$I_1(t^k;\Gamma) \approx I_{h1}^k := -\frac{\rho}{2}\int_\Gamma (\phi_h^k)|u_h^k|^2(u_h^k)\cdot n\,ds,$$

$$I_2(t^k;\Gamma) \approx I_{h2}^k := -\rho g \int_\Gamma (\phi_h^k)(\eta_h^k)(u_h^k)\cdot n\,ds,$$

$$I_3(t^k;\Gamma) \approx I_{h3}^k := 2\mu \int_\Gamma (\phi_h^k)(D(u_h^k)n)\cdot(u_h^k)\,ds,$$

$$I_4(t^k;\Omega) \approx I_{h4}^k := -2\mu \int_\Omega (\phi_h^k)|D(u_h^k)|^2\,dx.$$

Numerical simulations for the problem (2)—(5) with $L = 1, a = 0.1, u^0 = 0, c_1 = 0.001,\ p = (0.5, 0.5)^T$ are carried out by scheme (8) with $\Delta t = 2h$, $h = 0.007, 0.0047, 0.0035$ and 0.0028, where h is the maximum edge length of the triangle element.

3. Result and discussion

The results are presented in Figs. 3, 4 and 5, where (i)—(v) in the figures represent the cases (i)—(v) described in the subsection 2.1. The graphs of E_h^k and $\sum_{i=1}^4 I_{hi}^k$ versus $t = t^k (k \in \mathbb{N})$ are presented in the Figure 3 and Figure 4, respectively. There are four lines in each figure, but the lines are almost overlapped in the cases of (ii)—(v). In the case of (i) the graphs are qualitatively similar. The Figure 5 shows the graphs of $I_{hi}^k, i = 1, \dots, 4$ versus $t = t^k (k \in \mathbb{N})$ for $dt = 0.0056$ and $dx = 0.0028$. From the numerical results presented in Figure 3, it can be found that the total energy is mainly decreasing with respect to time. In the case of (i), i.e., $\Gamma = \Gamma_D$, we can see that the graphs are increasing in the Figure 3, while the values are small. We think this is because of numerical truncation error. But it can be seen that as the number of points in computation increases, the results seem to converge to a stable state. From the Figure 4 it can be clearly seen that the sum $\sum_{i=1}^4 I_{hi}^k$ corresponding to the derivative of the total energy is always non-positive, which confirms the stability of solutions to the model numerically.

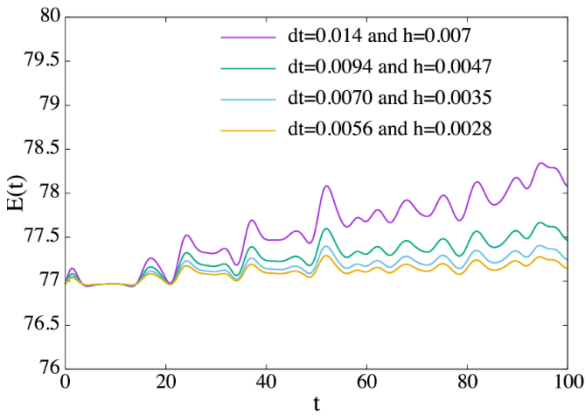

i

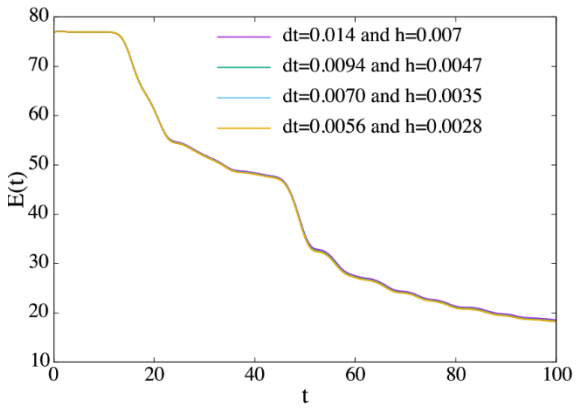

ii

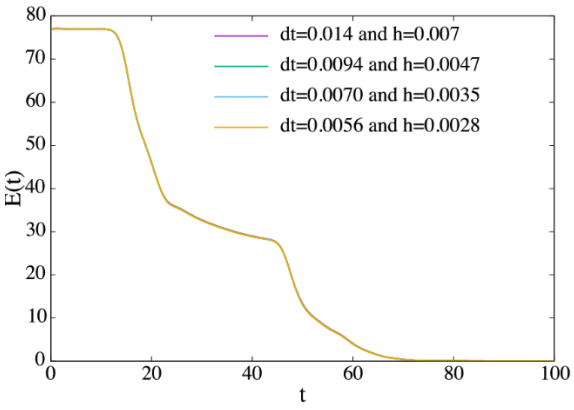

iii

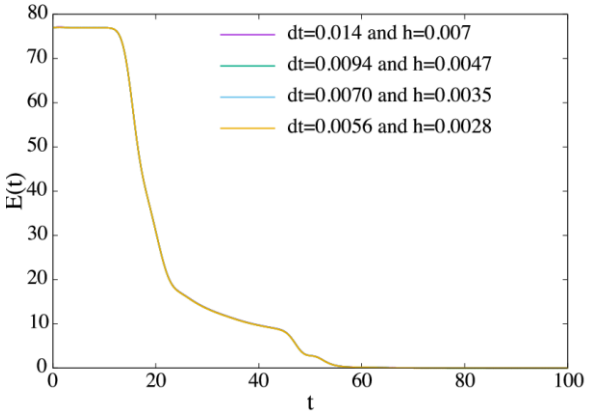

iv

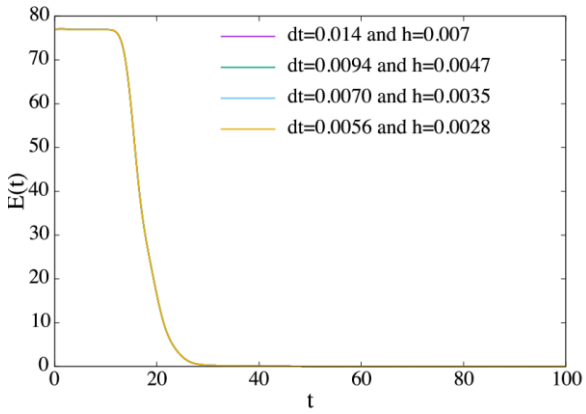

v

Figure 4 Graphs of E_h^k versus $t = t^k (\geq 0, k \in \mathbb{Z})$ for the five cases (i)—(v).

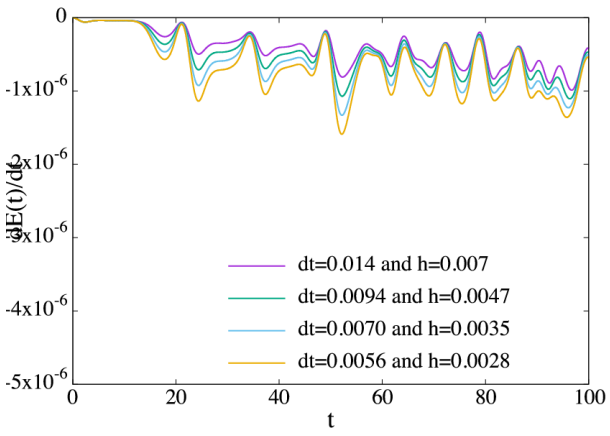

i

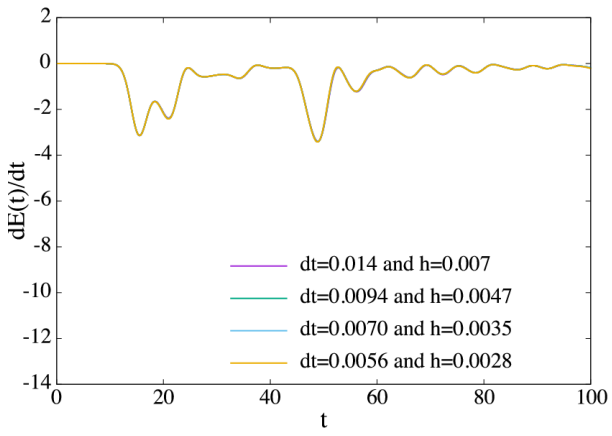

ii

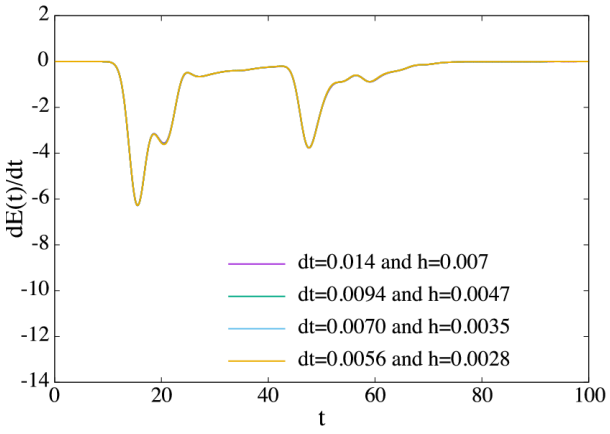

iii

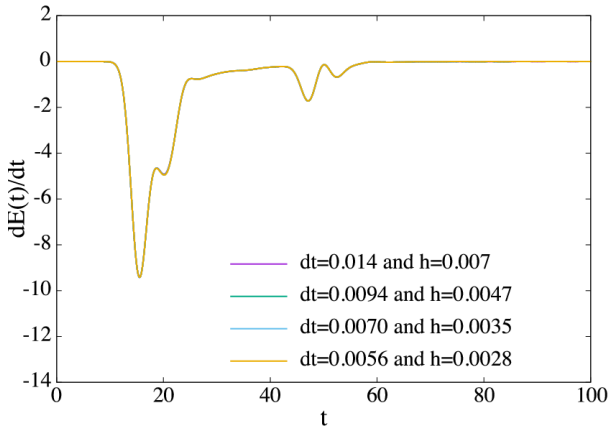

Iv

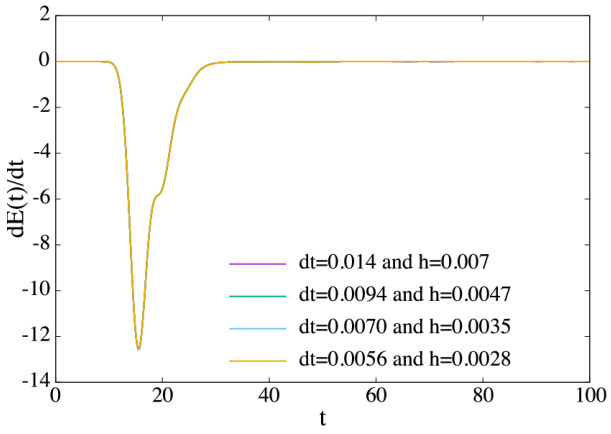

v

Figure 5 Graphs of $\sum_{i=1}^{4} I_{hi}^{k} \approx \frac{d}{dt}E(t)$ versus $t = t^{k} (\geq 0, k \in \mathbb{Z})$ for the five cases (i)—(v).

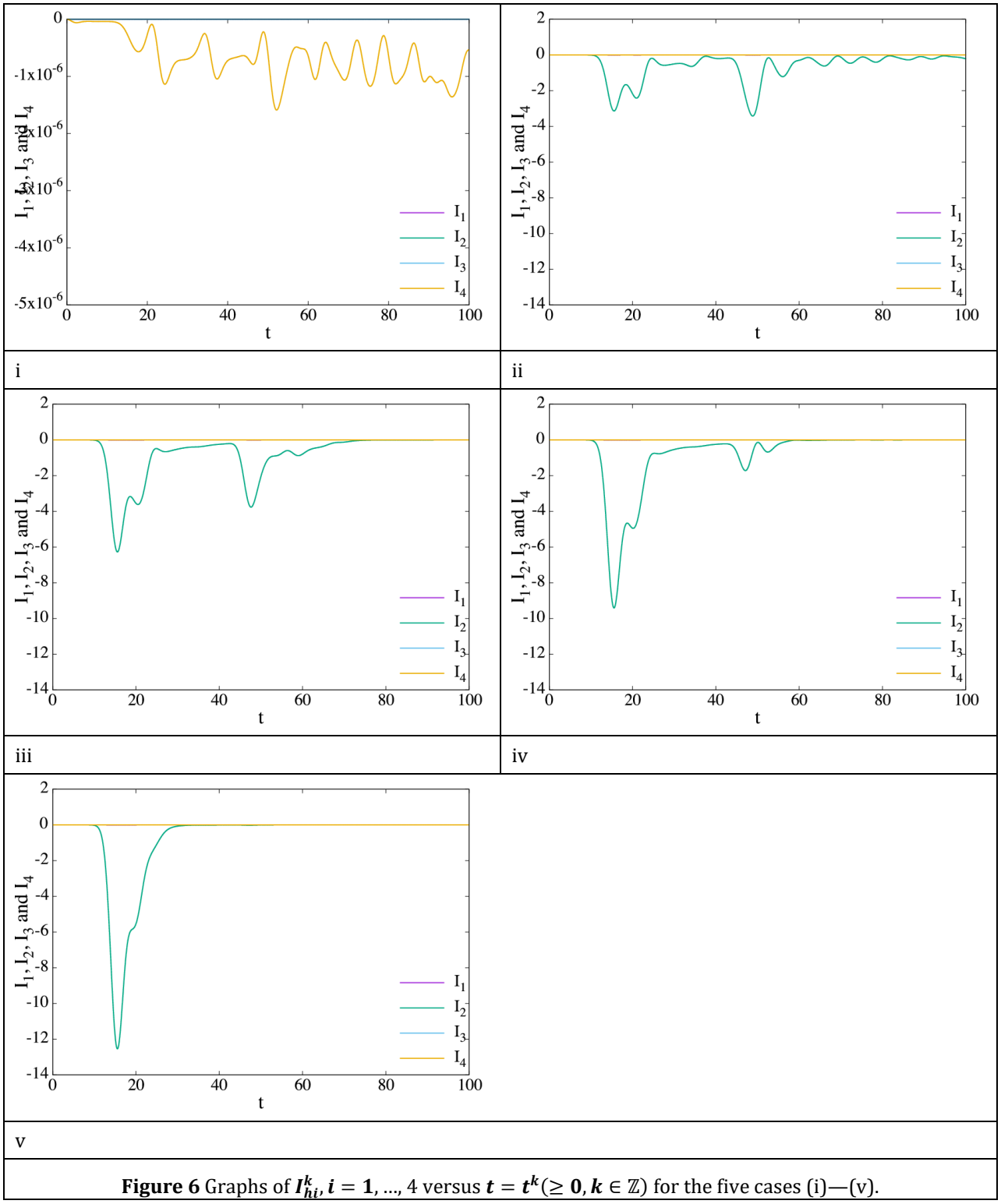

Figure 6 Graphs of $I_{hi}^{k}, i = 1, ..., 4$ versus $t = t^{k} (\geq 0, k \in \mathbb{Z})$ for the five cases (i)—(v).

4. Conclusion

This study analyzed the SWEs using a LG scheme with specified Dirichlet and transmission boundary conditions. The stability of the numerical solution was confirmed through energy estimates, which demonstrated that the total energy generally decreases over time, with non-positive energy derivatives. The results, particularly the consistency observed across different cases and the convergence towards a stable state as the number of computational points increased, validate the numerical stability of the model. These findings contribute valuable insights for the development of an efficient storm surge prediction model using the FEM.

Compliance with ethical standards

Acknowledgments

I appreciate the referees for their insightful comments and suggestions, which significantly improved this manuscript. I also extend my gratitude to Mr. Kouta Futai, Professor Masato Kimura, and Professor Hirofumi Notsu for their ongoing assistance in preparing the results.

Disclosure of conflict of interest

I declare no conflicts of interest.

References

[1] P. K. Das, Prediction model for storm surges in the Bay of Bengal, Nature, 239 (1972), 211—213.

[2] S. K. Debsarma, Simulations of storm surges in the Bay of Bengal, Marine Geodesy, 32 (2009), 178—198.

[3] B. Jonhs and A. Ali, The numerical modeling of storm surges in the Bay of Bengal, Quarterly Journal of the Royal Meteorological Society, 106 (1980), 1—18.

[4] H. Kanayama and H. Dan, Tsunami propagation from the open sea to the coast, Tsunami, Chapter 4, Intech Open, (2016), 61—72.

[5] M. M. Murshed, K. Futai, M. Kimura and H. Notsu (2021), Theoretical and numerical studies for energy estimates of the shallow water equations with a transmission boundary condition, Discrete Contin. Dyn. Syst. Ser. S. 14(3): 1063–1078.

[6] M. M. Rasid, M. Kimura, M. M. Murshed, E. R. Wijayanti and H. Notsu (2023), A Two-Step Lagrange–Galerkin Scheme for the Shallow Water Equations with a Transmission Boundary Condition and Its Application to the Bay of Bengal Region Part I: Flat Bottom Topography, Mathematics 11(7), 1633.

[7] G. C. Paul and A. I. M. Ismail, Tide surge interaction model including air bubble effects for the coast of Bangladesh, Journal of the Franklin Institute, 349 (2012), 2530—2546.

[8] G. C. Paul and A. I. M. Ismail, Contribution of o shore islands in the prediction of water levels due to tide-surge interaction for the coastal region of Bangladesh, Natural Hazards, 65 (2013), 13—25.

[9] G. C. Paul, A. I. M. Ismail and M. F. Karim, Implementation of method of lines to predict water levels due to a storm along the coastal region of Bangladesh, Journal of Oceanography, 70 (2014), 199—210.

[10] G. C. Paul, M. M. Murshed, M. R. Haque, M. M. Rahman and A. Hoque, Development of a cylindrical polar coordinates shallow water storm surge model for the coast of Bangladesh, Journal of Coastal Conservation, 21 (2017), 951—966.

[11] G. C. Paul, S. Senthilkumar and R. Pria, Storm surge simulation along the Meghna estuarine area: An alternative approach, Acta Oceanologica Sinica, 37 (2018), 40—49.

[12] G. C. Paul, S Senthilkumar and R. Pria, An efficient approach to forecast water levels owing to the interaction of tide and surge associated with a storm along the coast of Bangladesh, Ocean Engineering, 148 (2018), 516—529.

[13] G. D. Roy, A. B. M. Humayun Kabir, M. M. Mandal and M. Z. Haque, Polar coordinate shallow water storm surge model for the coast of Bangladesh, Dynamics of Atmospheres and Oceans, 29 (1999), 397—413.

[14] G. D. Roy and A. B. H. M. Kabir, Use of nested numerical scheme in a shallow water model for the coast of Bangladesh, BRAC University Journal, 1 (2004), 79—92.

[15] H. X. Rui and M. Tabata, A mass-conservative characteristic finite element scheme for convection-diffusion problems, Journal of Scientific Computing, 43 (2010), 416—432.